NASA TECHNICAL
MEMORANDUM

MEASUREMENTS OF THE STOCHASTIC NATURE OF ATMOSPHERIC SPECTRAL AMPLITUDES

By William C. Cliff, George H. Fichtl,
Margaret Alexander, and Salvador Arias
Space Sciences Laboratory

August 1976

NASA

George C. Marshall Space Flight Center

Marshall Space Flight Center, Alabama

1. REPORT NO. NASA TM X-73329	2. GOVERNMENT ACCESSION NO.	3. RECIPIENT'S CATALOG NO.
4 TITLE AND SUBTITLE Measurements of the Stochastic Nature of Atmospheric Spectral Amplitudes		5. REPORT DATE August 1976
		6. PERFORMING ORGANIZATION CODE
7. AUTHOR(S) William C. Cliff, George H. Fichtl, Margaret Alexander, and Salvador Arias		8. PERFORMING ORGANIZATION REPORT #
9. PERFORMING ORGANIZATION NAME AND ADDRESS George C. Marshall Space Flight Center Marshall Space Flight Center, Alabama 35812		10. WORK UNIT NO.
		11. CONTRACT OR GRANT NO.
12 SPONSORING AGENCY NAME AND ADDRESS National Aeronautics and Space Administration Washington, D.C. 20546		13. TYPE OF REPORT & PERIOD COVERED Technical Memorandum
		14. SPONSORING AGENCY CODE

15. SUPPLEMENTARY NOTES

16. ABSTRACT

The stochastic nature of the power spectral amplitudes of the neutral atmospheric boundary layer is examined. Probability density distributions and probability distributions of longitudinal and lateral power spectral amplitudes are computed from neutral atmospheric boundary layers at Cape Kennedy. The statistical distributions are computed for frequencies of 0.006, 0.01, 0.03, 0.06, 0.1, and 0.5 Hz at each of the elevations of 18, 30, 60, 90, 120, and 150 m. When the probability density distributions are properly nondimensionalized, the data tend to collapse to a universal curve. An empirical curve fit to the universal nondimensionalized probability density distribution is also given. Probability distributions of individual frequency power spectral amplitudes are also presented for all elevations and frequencies.

An interesting observation from the data is that greater than 10 percent of the time the power spectral amplitude at a given frequency will generally be more than three times the temporal mean value computed by standard Fourier techniques. The standard power spectral density curves are also included in the report.

17. KEY WORDS	18. DISTRIBUTION STATEMENT *William C. Cliff* Unclassified — Unlimited

19. SECURITY CLASSIF. (of this report) Unclassified	20 SECURITY CLASSIF. (of this page) Unclassified	21. NO. OF PAGES 33	22. PRICE NTIS

MSFC - Form 3292 (Rev December 1972)   For sale by National Technical Information Service, Springfield, Virginia 22151

TABLE OF CONTENTS

LIST OF ILLUSTRATIONS

LIST OF ILLUSTRATIONS (Continued)

LIST OF ILLUSTRATIONS (Concluded)

MEASUREMENTS OF THE STOCHASTIC NATURE OF ATMOSPHERIC SPECTRAL AMPLITUDES

INTRODUCTION

In 1915, G. I. Taylor [1] first examined eddy motion in the atmosphere, and in 1917 [2] he performed experiments to map the shape of eddies in the atmosphere. In 1938, Taylor [3] published the relationship between correlation measurements and spectra (harmonic analyses) to statistically analyze an atmospheric velocity record. Since that time, harmonic analysis has been the standard technique to statistically compress velocity records. The relationship of the harmonic amplitudes of the velocity record to that of the harmonic amplitudes representing the autocorrelation is given in other works [4]. The objective of this report is to specifically address the stochastic nature of these harmonic amplitudes (i.e., the stochastic nature of the power spectral amplitudes of wind records). The general statistical technique for analyzing a wind record is to take a wind velocity record and perform the standard Fourier decomposition of the data record given by:

$$R_{uu}(\tau) = \frac{1}{T} \int_0^T u(t)\, u(t+\tau)\, dt \tag{1}$$

and

$$R_{uu}(\tau) = \frac{1}{2\pi} \int_{-\infty}^{\infty} C(\omega)\, e^{i\omega\tau}\, d\omega$$

where

$$C(\omega) = \int_{-\infty}^{\infty} R_{uu}(\tau)\, e^{-i\omega\tau}\, d\tau \tag{2}$$

and where $R_{uu}(\tau)$ is the time averaged autocorrelation of the u component of velocity and $C(\omega)$ is the average power spectral amplitude at a frequency, ω. It is well understood, however, that even under neutral atmospheric conditions the value of statistical measures of the atmospheric winds are stochastic and thus depend to some degree upon the integration time or observation time from which the statistic is evaluated. Thus, by allowing the power spectral amplitude to be a function of time as well as frequency, one is able to develop the statistical properties of $C(\omega,t)$ such that

$$C(\omega) = \frac{1}{T} \int_0^T C(\omega,t)\, dt \qquad . \tag{3}$$

PROCEDURE

The technique used here to evaluate $C(\omega,t)$ was to first select long time histories of neutral atmospheric wind velocities. These time histories were filtered at a desired frequency; the filtered function was then squared and divided by twice the filter bandwidth. The peaks of the resulting time function now correspond to a temporal record of the power spectral amplitudes of the original data record; that is, the peaks represent $C(\omega,t)$, where

$$C(\omega,t) = \frac{A^2(\omega,t)}{2\Delta B}$$

and where $A(\omega,t)$ is the temporal Fourier amplitude of the wind record, such that

$$C(\omega) = \frac{1}{T} \int_0^T C(\omega,t)\, dt = \frac{1}{T} \int_0^T \frac{A^2(\omega,t)}{2\Delta B}\, dt \qquad . \tag{4}$$

As expected, equation (4) simply states that the general power spectral amplitude is equal to the time averaged stochastic power spectral amplitude.

The power spectral amplitude, $C(\omega,t)$, may be represented by the well known relationship between power spectral amplitude and its frequency complement in Fourier representation of the original velocity time history.

RESULTS

Using the technique outlined in the previous section, the probability density distribution (PDD) of the power spectra for individual frequency components are computed from temporal wind records of five neutral atmospheric boundary layers. Longitudinal and lateral wind components are analyzed at frequencies of 0.006, 0.01, 0.03, 0.06, 0.1, and 0.5 Hz from data records taken at elevations of 18, 30, 60, 90, 120, and 150 m. All corresponding standard statistical measurements are also included. A typical example of the calculated longitudinal wind component power spectra is presented in Figure 1.

The main objective of this report, as noted previously, is to examine the stochastic nature of the power spectra amplitude for individual frequency components. The stochastic nature of the individual frequency spectral amplitudes is presented in the form of PDD. The PDD of an individual frequency is presented in Figure 2. Figure 2 is the PDD of the longitudinal wind component for a frequency of 0.06 Hz and the data taken at an elevation of 18 m. Figure 2 is taken from the same data record as Figure 1. Thus, the mean value of the power spectral amplitude from Figure 2,

$$C(\omega) = C(\omega,t) = \int_{-\infty}^{\infty} C(\omega,t)\, P(C(\omega,t))\, d\, C(\omega,t) \quad,$$

must be equivalent to the ensemble mean value (Fig. 1) which was calculated by conventional harmonic analysis. The two values are seen to be equivalent. It is interesting to note that because the power spectra amplitude is always positive (which results in a natural skewing), the rms value of the amplitudes can easily be larger than the mean value. For the case in Figure 2, the mean value is approximately 10, whereas the rms value of the same curve has a value greater than 13. Because the PDD of the power spectra components is always positive, it is tempting to speculate that the PDD could be approximated by standard statistical distributions such as the gamma, exponential, or beta. An empirical curve fit to the data taken is presented later. The density distribution appears to have a negative exponential form.

Figure 3 presents the probability distribution (PD) for the same data as used to compute Figures 1 and 2. An interesting observation from Figure 3 is that greater than 10 percent of the probability curve lies beyond a value three times that of the mean value.

Similarity techniques are used here to collapse the PDD of all frequencies (of a given wind direction and elevation) to a single curve. The collapse of the normalized PDD for the power spectral amplitude of the longitudinal component for several frequencies taken at an elevation of 18 m is presented in Figure 4, while an example of the collapse of 1.0 minus the PD for the same data is given in Figure 5.

The PDD and PD of the raw data amplitudes for individual frequencies and the PDD and PD of the power spectral amplitudes for individual frequencies were computed. These amplitudes appeared to be symmetrical with the PDD and PD of the negative amplitudes which were assumed to be mirror images of the positive PDD and PD; thus, only positive amplitudes were computed. An example of the PDD of the raw data amplitudes for various frequencies is presented in Figure 6.

Plots of the normalized PDD of the frequency-dependent longitudinal power spectral amplitudes of data taken at elevations 30, 60, 90, 120, and 150 m are presented in Figures 7 through 11, respectively. Plots of the normalized PDD of the frequency-dependent lateral power spectra amplitudes of data taken at elevations of 18, 30, 60, 90, 120, and 150 m are presented in Figures 12 through 17, respectively.

Figures 18 through 22 present the standard power spectral density curves of the longitudinal wind component for elevations 30, 60, 90, 120, and 150 m, respectively. Note that the value taken from these curves at a given frequency is the mean value of the stochastic power spectral amplitude and is denoted $C(\omega)_m$.

Figures 23 through 28 present the standard power spectral density curves of the lateral wind component for elevations of 18, 30, 60, 90, 120, and 150 m, respectively. Again, as was previously the case, a value taken from these curves represents the mean value of the stochastic power spectral amplitude which is denoted as $C(\omega)_m$.

The most interesting observation from this collection of data is that all of the normalized probability density curves of the power spectral amplitudes (whether of the longitudinal or lateral component, and independent of the

4

elevation at which the data were taken and independent of the frequency of concern) appear to collapse to a universal curve which may be expressed as

$$\frac{P(C(\omega,t))}{P(C(\omega)_m)} = e^{-x^{0.8}+1} + 30.25 \, e^{-20x} \qquad \text{for} \quad x > 0 \qquad (5)$$

$$= 0 \qquad \qquad \text{for} \quad x < 0$$

where

$$x = \frac{C(\omega,t)}{C(\omega)_m}$$

and where $P(C(\omega,t))$ is the value of the PDD for a given amplitude $C(\omega,t)$, $P(C(\omega)_m)$ is the value of the PDD of the average power spectral density, $C(\omega,t)$ is the given amplitude, and $C(\omega)_m$ is the average amplitude taken directly from the standard power spectral density curve.

Equation (5) then leads to formulation of an empirical PDD for $C(\omega,t)/C(\omega)_m$ by simply dividing equation (5) by the area under the curve. Thus,

$$P\left(\frac{C(\omega,t)}{C(\omega)_m}\right) = P(x) = \frac{e^{-x^{0.8+1}} + 30.25 \, e^{-20x}}{4.592} \qquad \text{for} \quad x \geq 0 \quad (6)$$

$$= 0 \qquad \qquad \text{for} \quad x < 0$$

where

$$X = \frac{C(\omega,t)}{C(\omega)_m} \qquad .$$

It should be noted that

$$\int_{-\infty}^{\infty} P(x)\, dx = 1$$

and also that

$$\overline{X} = \int_{-\infty}^{\infty} x\, P(x)\, dx = 1 \quad .$$

The second equation results from the requirement that

$$\frac{1}{T} \int_{-\infty}^{\infty} C(\omega, t) = C(\omega)_m \quad .$$

Equation (6) conforms to both of these requirements. A plot of equation (6) is presented in Figure 29, and tabular results are given in the Table. Other curves which may interest a designer are curves representing the distribution of the variance of the spectral amplitudes [i.e., $X^2\, P(x)$] and the distribution of the mean spectral values [i.e., $x\, P(x)$]. These curves are presented in Figures 30 and 31, respectively, to show what values of spectral amplitude contribute to the value and mean value of spectral amplitudes. Another obvious curve of interest to the designer is the probability distribution curve, that is, the integral of the probability density distribution. The empirical probability distribution curve resulting from equation (6) is presented graphically in Figure 32 and in tabular form in the Table. From the Table it is interesting to note that approximately 9 percent of the fluctuations are greater than three times the mean spectral amplitude. This value is found by looking at $X = 0$ and the corresponding value of $\int_{0}^{X} P(x)\, dx$ from the Table.

6

CONCLUSIONS

The stochastic nature of power spectral amplitudes for neutral atmospheric boundary layers has been studied. ̄ ͻ study shows that the PDD of the spectral amplitudes monotonically decreases for increasing amplitude. Because of the natural skewing of the PDD, the rms value (standard deviation) may be larger than the mean value. Approximately 10 percent of the expected instantaneous power spectral amplitudes has been shown to exceed a value greater than three times the mean value. Perhaps the most significant contribution is that the PDD of the spectral amplitudes will collapse to a universal curve. This curve is independent of whether the longitudinal or lateral wind component is analyzed, independent of the specific frequency analyzed, and independent of the elevation at which the atmospheric wind record was taken.

TABLE. VALUES OF THE PROBABILITY AND PROBABILITY DENSITY DISTRIBUTION OF POWER SPECTRAL AMPLITUDES

$$X = \frac{C(\omega,t)}{C(\omega)_m} \quad ; \quad P(x) = \frac{e^{-x^{0.8}+1} + 30.25e^{-20x}}{4.592}$$

$$\bar{X} = \int_0^\infty x\,P(x)\,dx = 1 \quad ; \quad \int_0^\infty P(x)\,dx = 1$$

| X	P(x)	$\int_0^x P(x)dx$	X	P(x)	$\int_0^x P(x)dx$
.10	1.41086	.33902	3.60	.03686	.93670
.20	.57564	.42516	3.70	.03466	.94024
.30	.42473	.47297	3.80	.03259	.94356
.40	.37207	.51213	3.90	.03066	.94669
.50	.33699	.54716	4.00	.02885	.94964
.60	.30769	.57903	4.10	.02716	.95241
.70	.28196	.60819	4.20	.02557	.95502
.80	.25904	.63495	4.30	.02408	.95747
.90	.23849	.65955	4.40	.02269	.95979
1.00	.21997	.68223	4.50	.02138	.96197
1.10	.20322	.70316	4.60	.02015	.96402
1.20	.18801	.72251	4.70	.01900	.96596
1.30	.17416	.74043	4.80	.01792	.96779
1.40	.16152	.75703	4.90	.01691	.96951
1.50	.14996	.77244	5.00	.01595	.97114
1.60	.13936	.78675	5.10	.01505	.97267
1.70	.12963	.80006	5.20	.01421	.97412
1.80	.12068	.81244	5.30	.01342	.97549
1.90	.11244	.82398	5.40	.01267	.97678
2.00	.10484	.83472	5.50	.01197	.97800
2.10	.09782	.84475	5.60	.01131	.97915
2.20	.09133	.85411	5.70	.01069	.98023
2.30	.08533	.86285	5.80	.01010	.98126
2.40	.07976	.87102	5.90	.00955	.98224
2.50	.07460	.87865	6.00	.00903	.98315
2.60	.06981	.88580	6.10	.00854	.98402
2.70	.06537	.89249	6.20	.00807	.98485
2.80	.06123	.89875	6.30	.00764	.98562
2.90	.05739	.90462	6.40	.00723	.98636
3.00	.05380	.91012	6.50	.00684	.98706
3.10	.05047	.91528	6.60	.00647	.98771
3.20	.04736	.92012	6.70	.00613	.98834
3.30	.04446	.92466	6.80	.00580	.98893
3.40	.04175	.92893	6.90	.00550	.98949
3.50	.03922	.93293	7.00	.00521	.99002
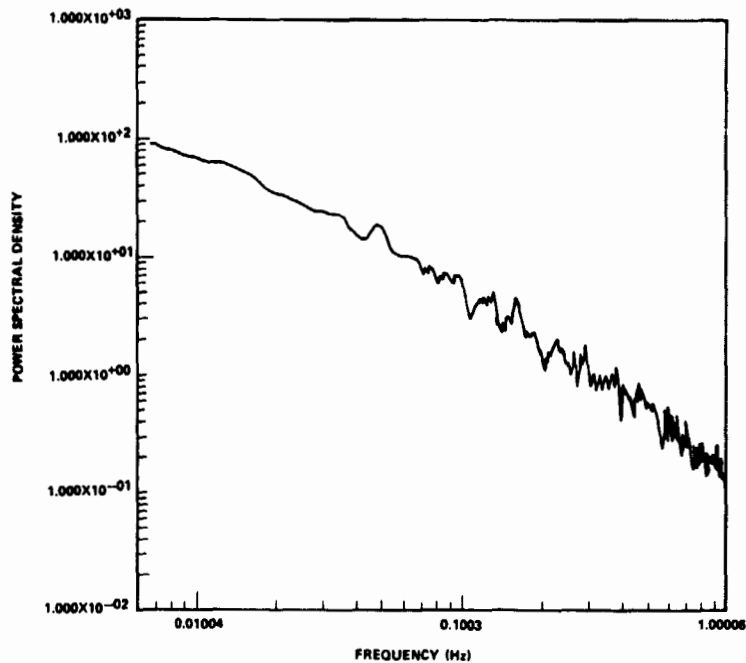
Figure 1. Power spectral density of longitudinal wind component
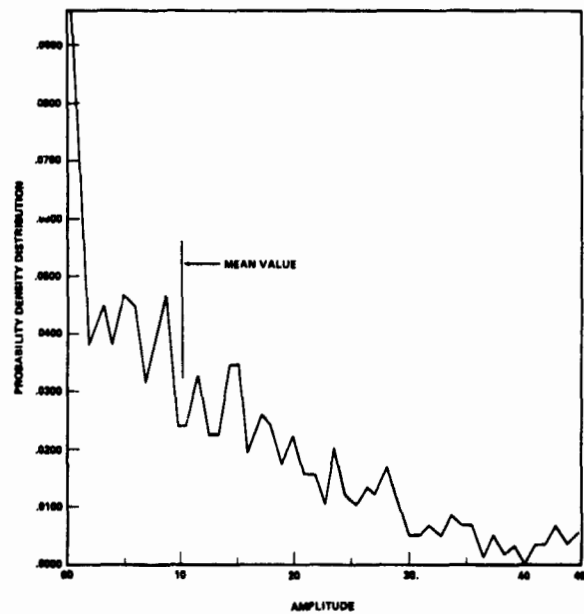(data taken at an elevation of 18 m, rms = 1.89 m/s).

Figure 2. Probability density distribution of the longitudinal power
spectral amplitudes for a frequency of 0.06 Hz
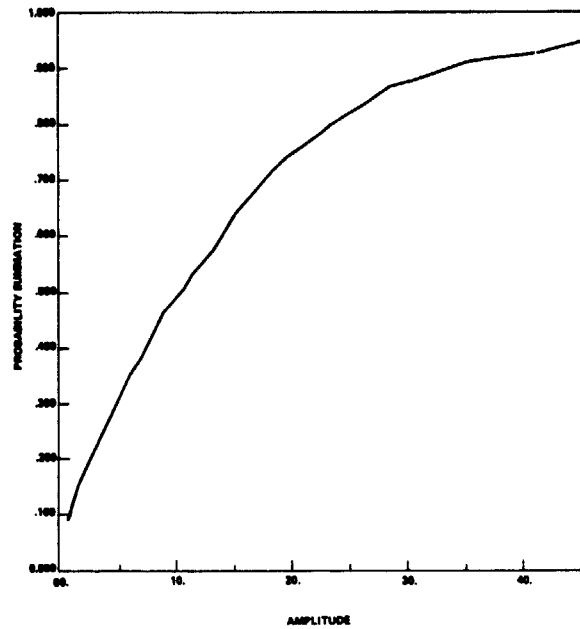(data taken at an elevation of 18 m).

9

Figure 3. Probability distribution of the longitudinal power spectral
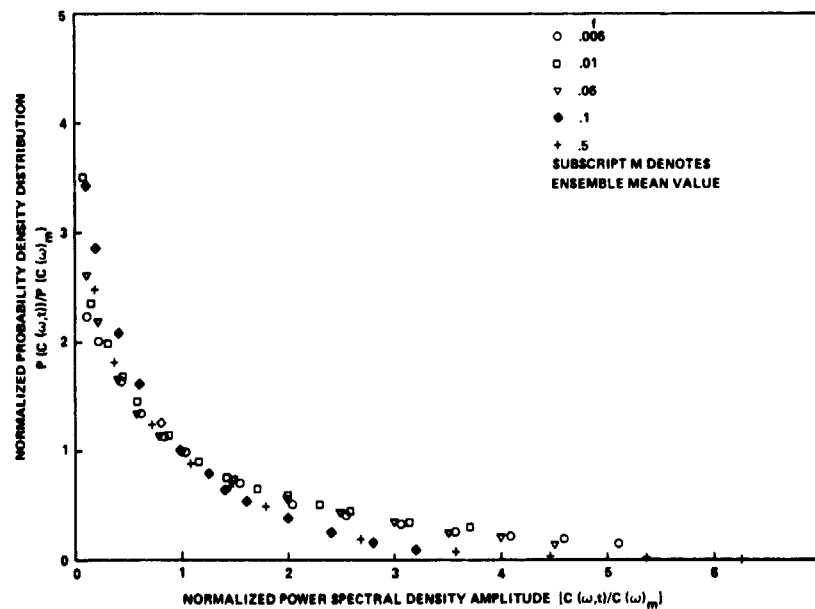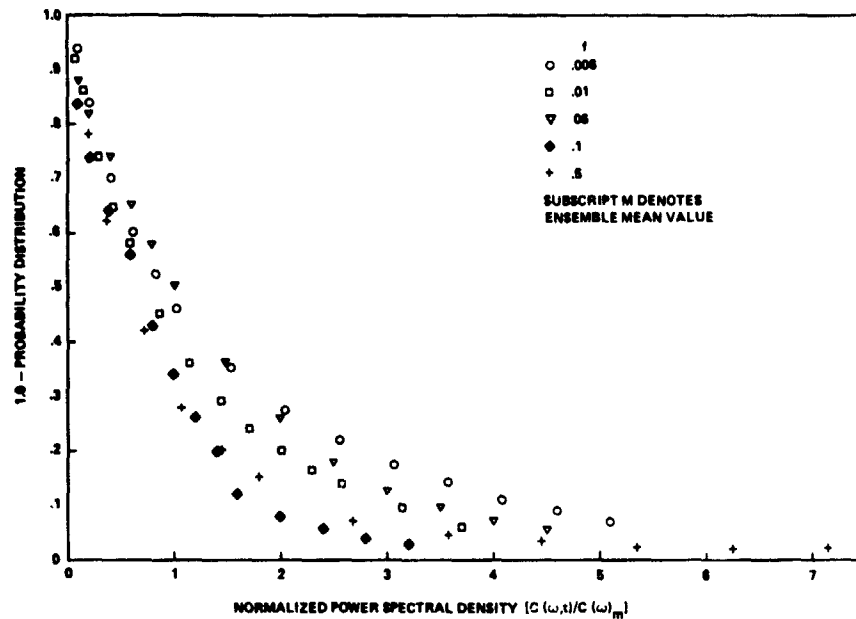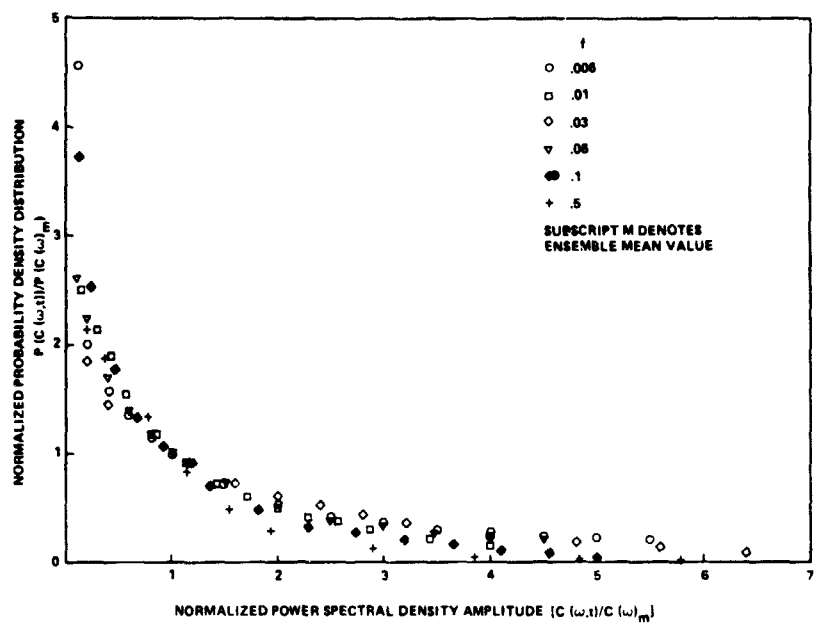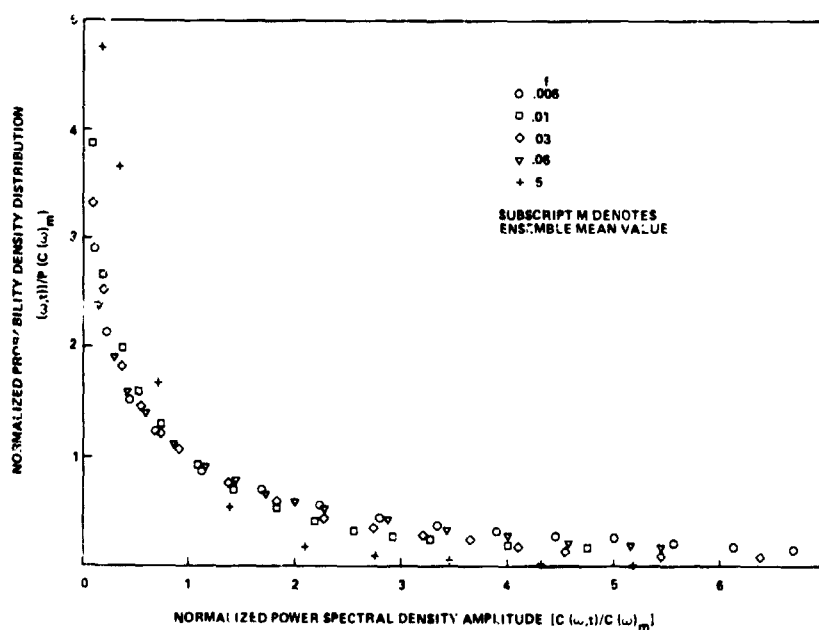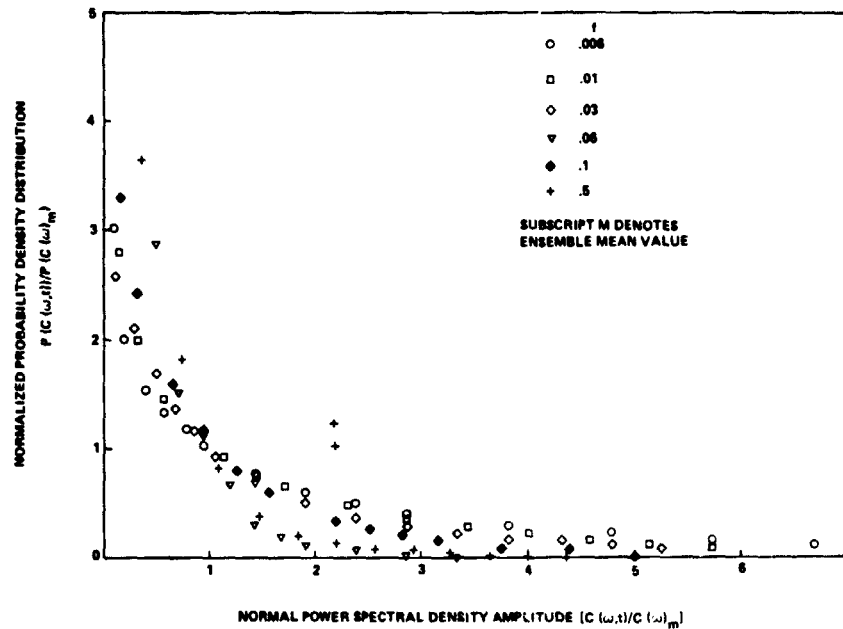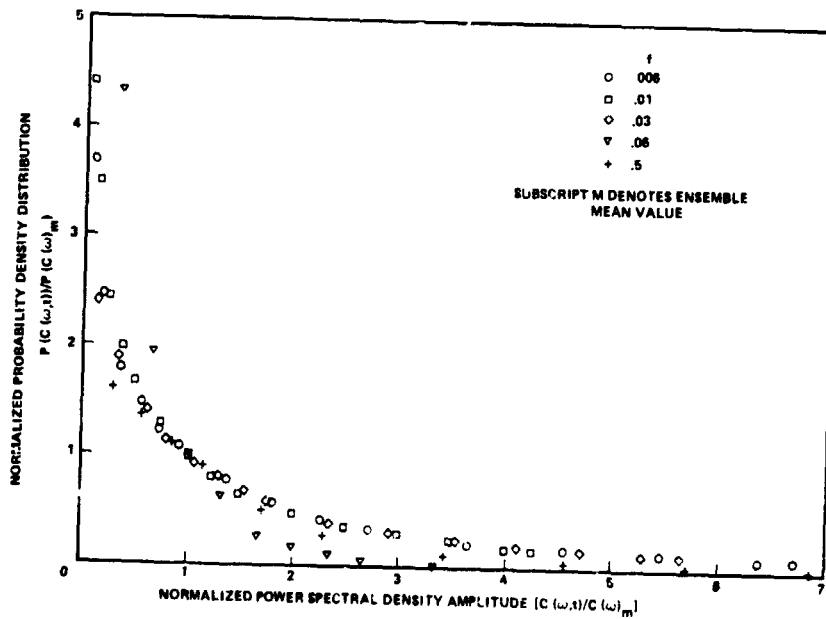amplitudes for a frequency of 0.06 Hz (data taken at an
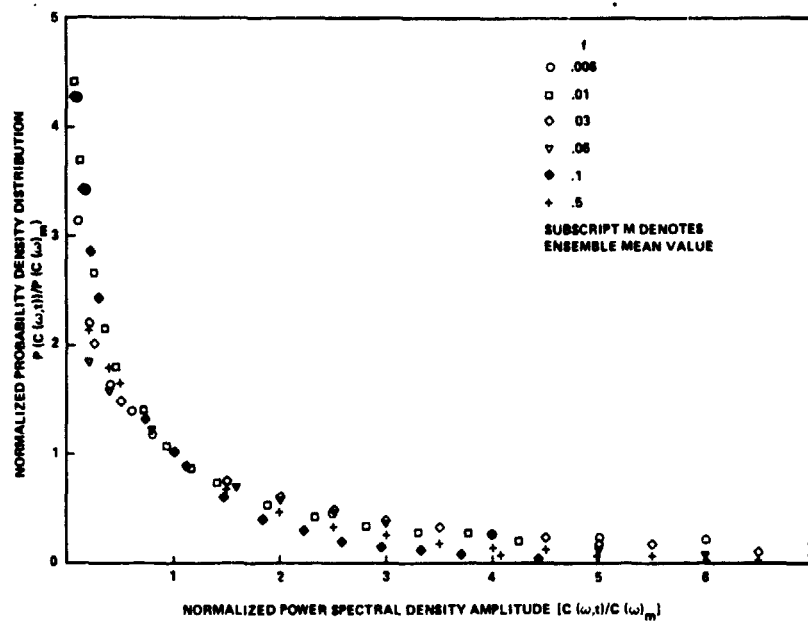elevation of 18 m).

Figure 4. Comparison of probability density distribution of longitudinal
power spectral amplitudes for various frequencies
(data taken at an elevation of 18 m).

10

Figure 5. Comparison of 1.0 probability density distribution versus amplitude for various frequencies (data are of the longitudinal wind component taken at an elevation of 18 m).
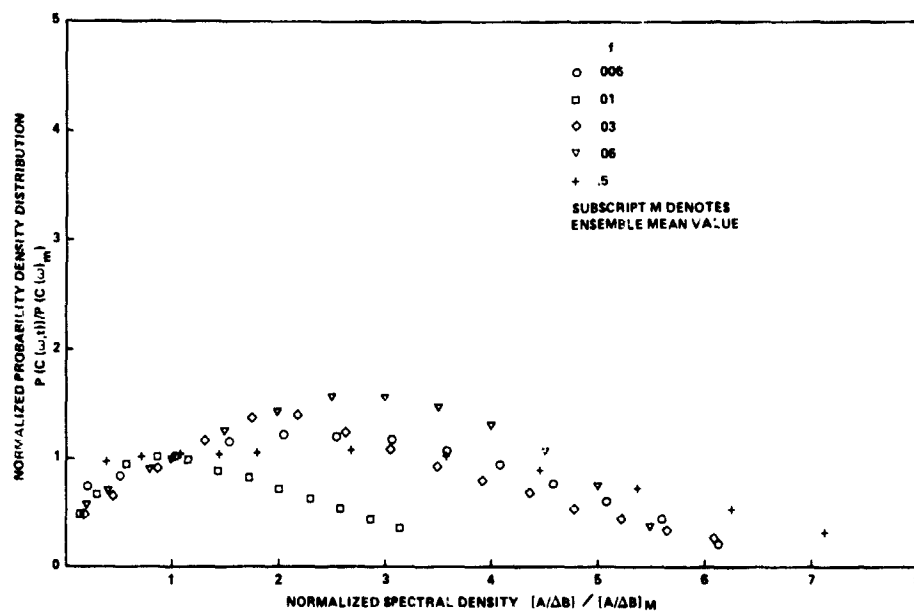
Figure 6. Comparison of the probability density distribution of the raw data amplitudes for various frequencies (data are of the longitudinal wind component taken at an elevation of 18 m).

11

Figure 7. Probability density distribution of longitudinal power spectral amplitudes for various frequencies (data taken at an elevation of 30 m).
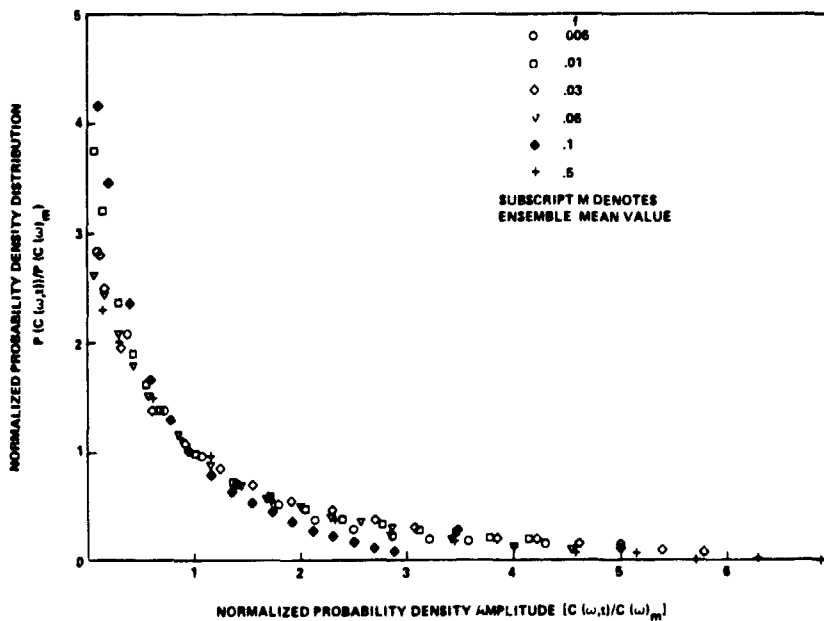
Figure 8. Probability density distribution of longitudinal power spectral amplitudes for various frequencies (data taken at an elevation of 60 m).
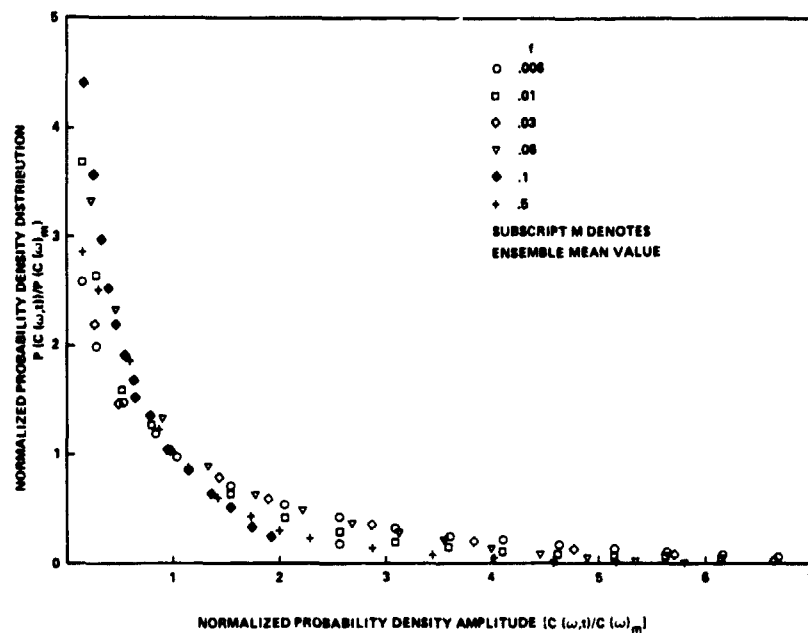
Figure 9. Probability density distribution of longitudinal power spectral amplitudes for various frequencies (data taken at an elevation of 90 m).
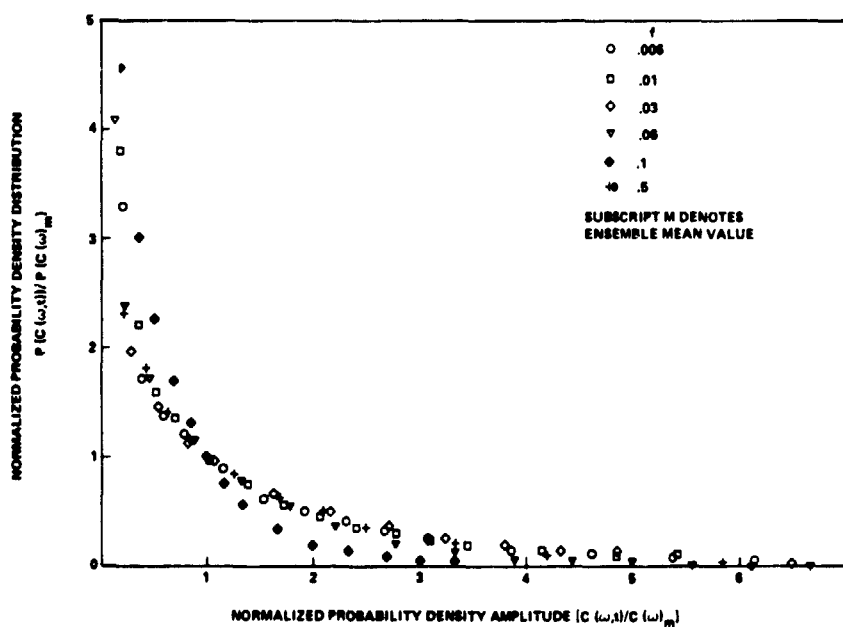

Figure 10. Probability density distribution of longitudinal power spectral amplitudes for various frequencies (data taken at an elevation of 120 m).

13

Figure 11. Probability density distribution of longitudinal power spectral
amplitudes for various frequencies (data taken at an elevation of 150 m).
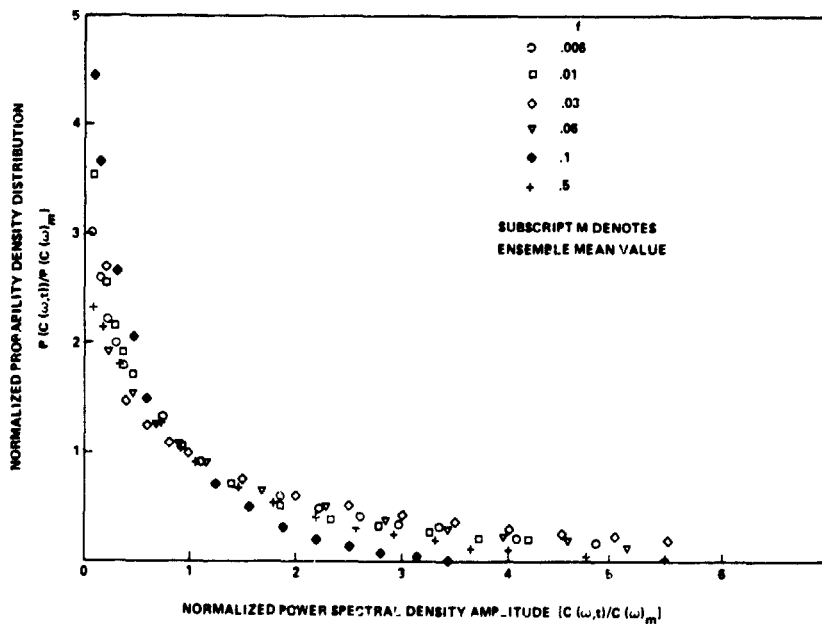
Figure 12. Probability density distribution of lateral power spectral amplitudes
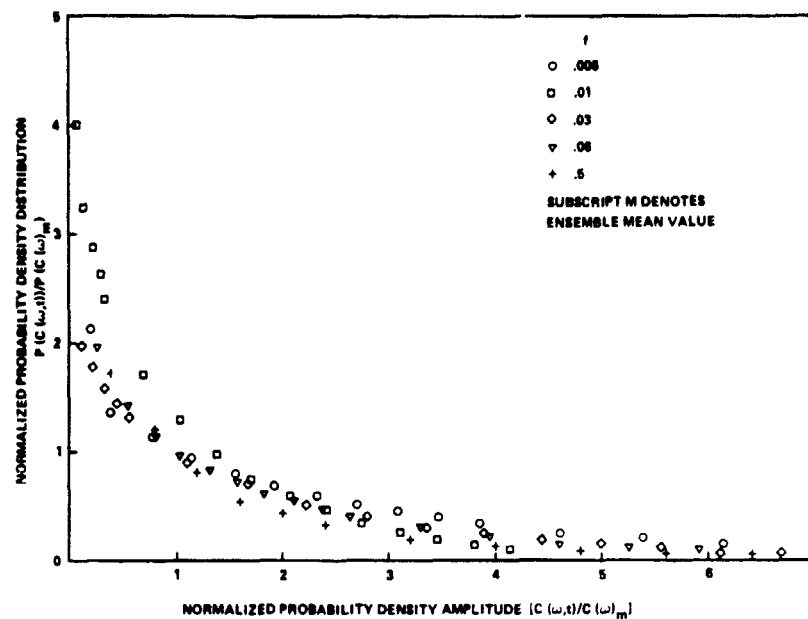for various frequencies (data taken at an elevation of 18 m).

14
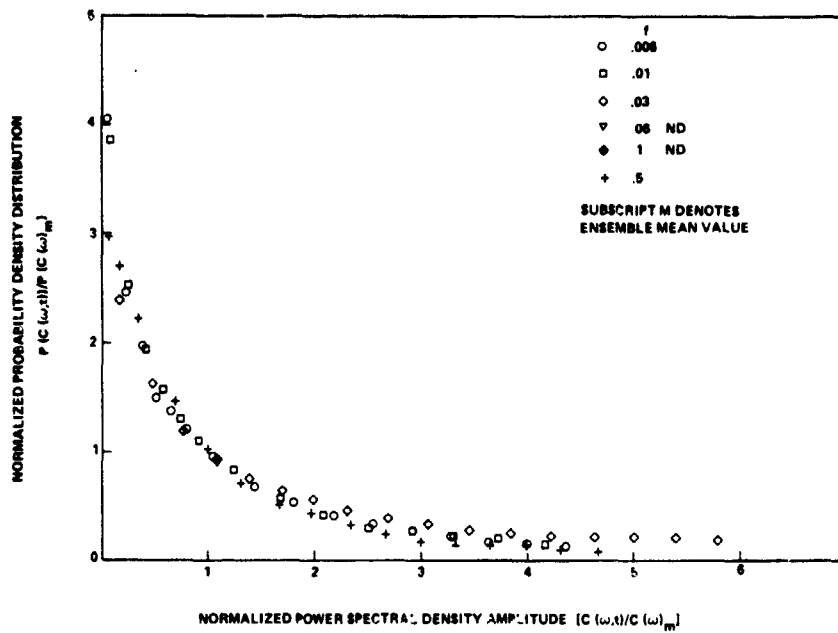
Figure 13. Probability density distribution of lateral power spectral amplitudes for various frequencies (data taken at an elevation of 30 m).

Figure 14. Probability density distribution of lateral power spectral amplitudes for various frequencies (data taken at an elevation of 60 m).

15

Figure 15. Probability density distribution of lateral power spectral amplitudes
for various frequencies (data taken at an elevation of 90 m).

Figure 16. Probability density distribution of lateral power spectral amplitudes
for various frequencies (data taken at an elevation of 120 m).

16

Figure 17. Probability density distribution of lateral power spectral
amplitudes for various frequencies (data taken at
an elevation of 150 m).
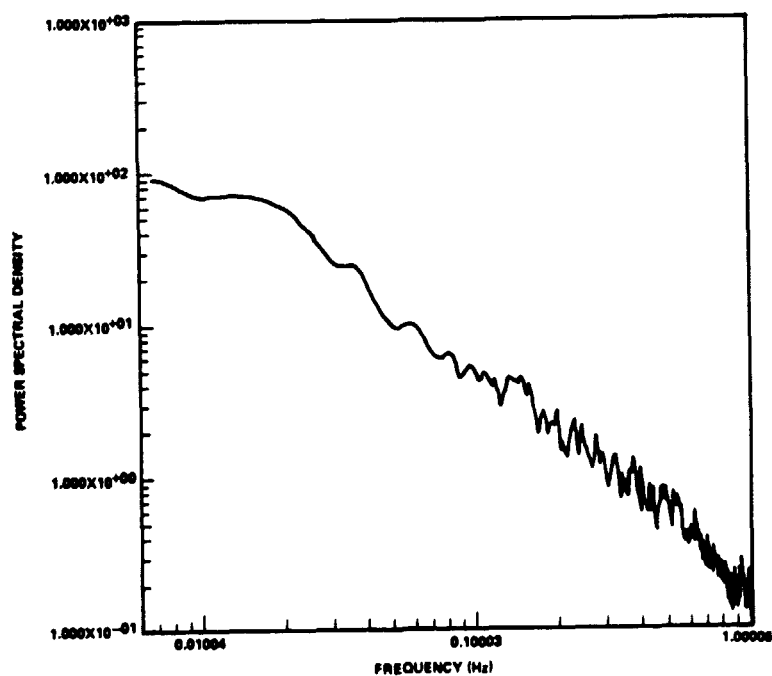
Figure 18. Power spectral density of longitudinal wind component
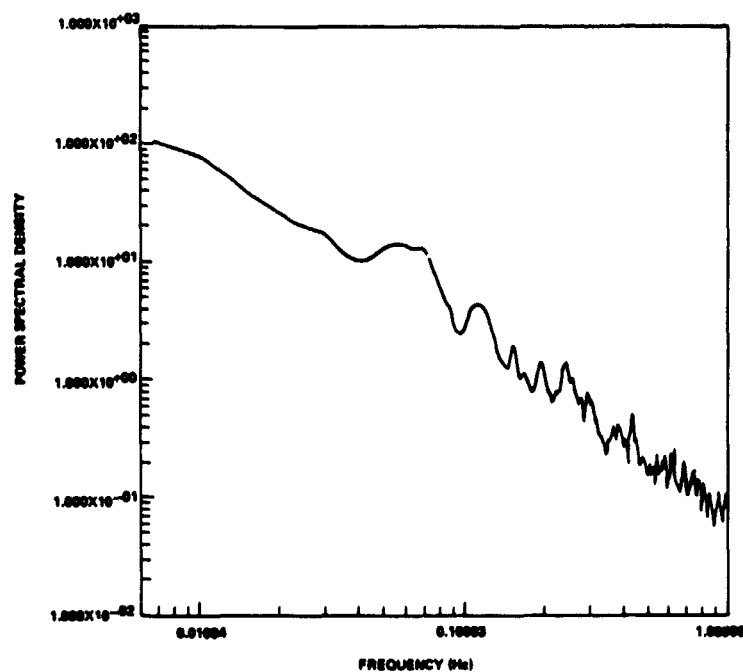(data taken at an elevation of 30 m, rms = 1.93 m/s).

17
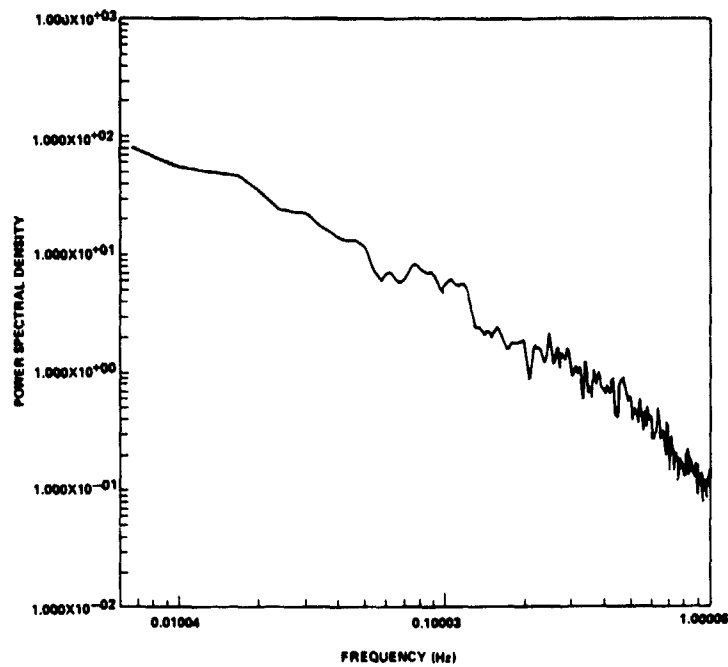
Figure 19. Power spectral density of longitudinal component (data
taken at an elevation of 60 m, rms = 1.79 m/s).
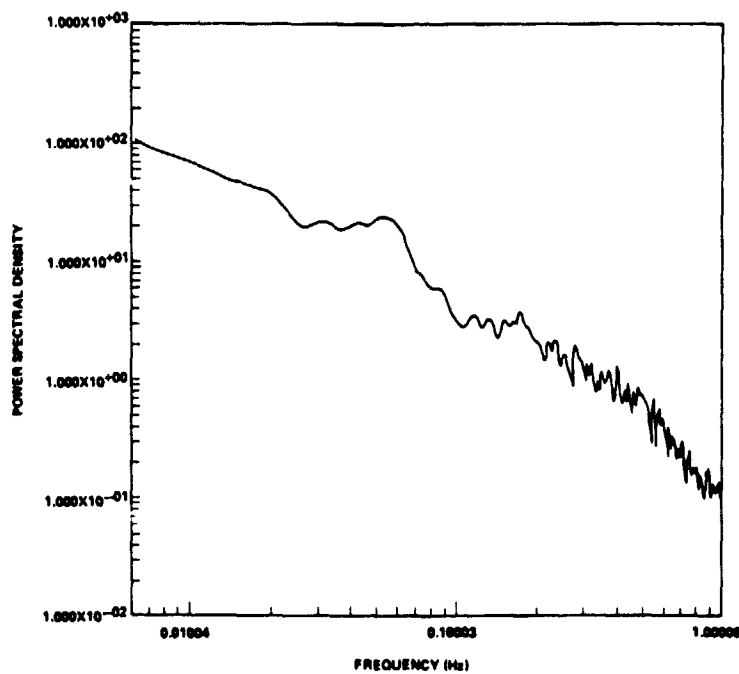
Figure 20. Power spectral density of longitudinal component (data
taken at an elevation of 90 m, rms = 1.90 m/s).

18

Figure 21. Power spectral density of longitudinal component (data taken at an elevation of 120 m, rms = 1.66 m/s).
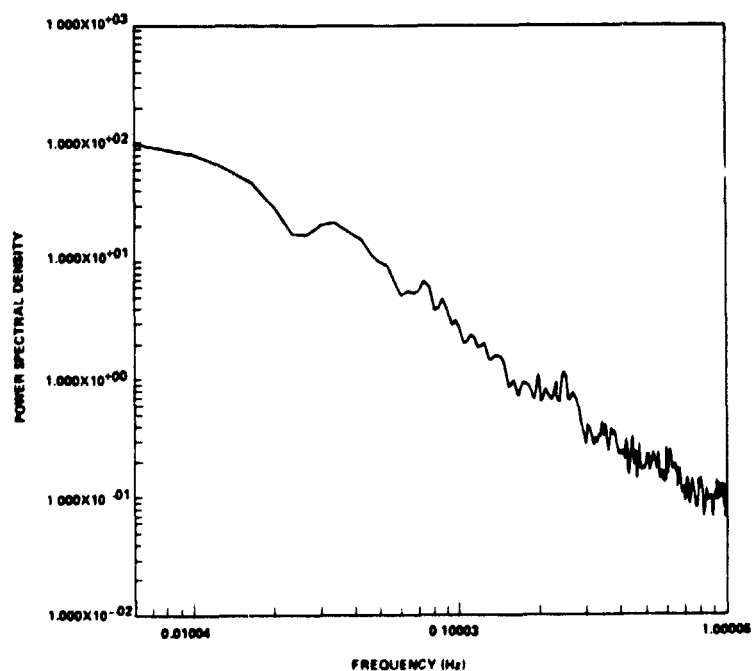

Figure 22. Power spectral density of longitudinal component (data taken at an elevation of 150 m, rms = 1.63 m/s).
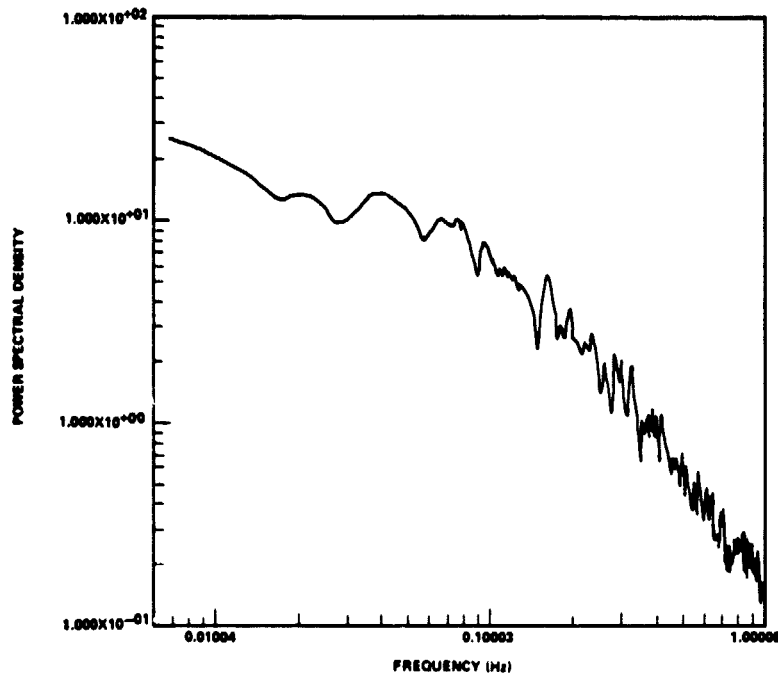
Figure 23. Power spectral density of lateral component (data
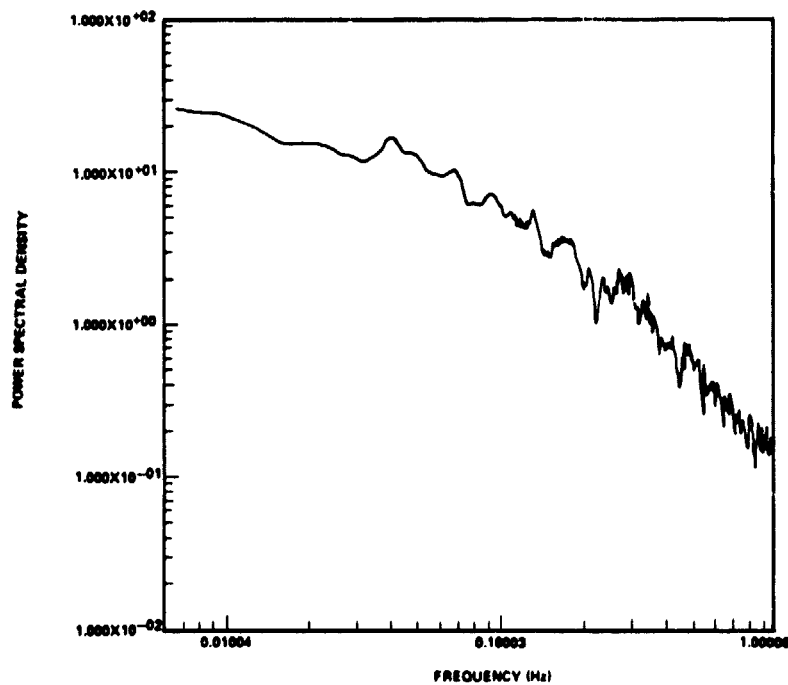taken at an elevation of 18 m, rms = 1.48 m/s).

Figure 24. Power spectral density of lateral component (data
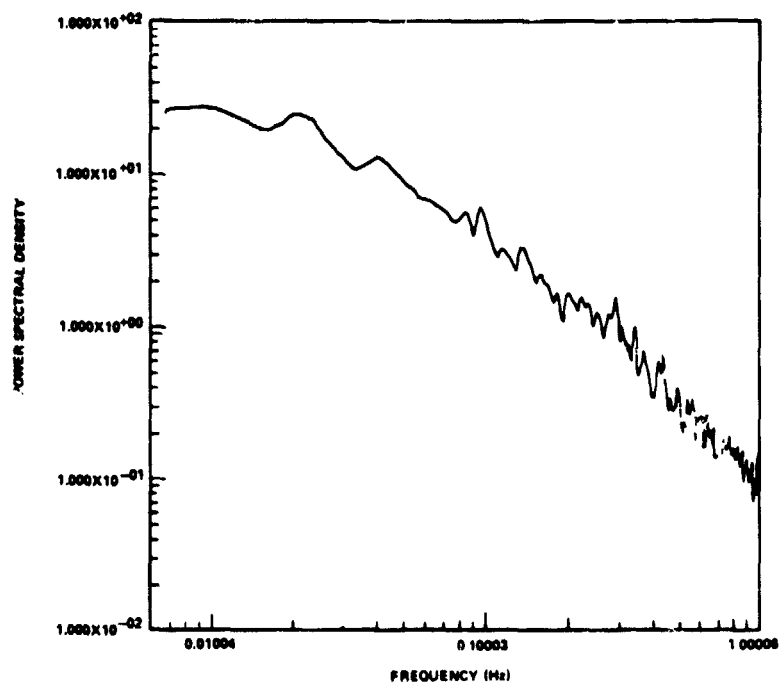taken at an elevation of 30 m, rms = 1.48 m/s).

Figure 25. Power spectral density of lateral component (data taken at an elevation of 60 m, rms = 1.35 m/s).
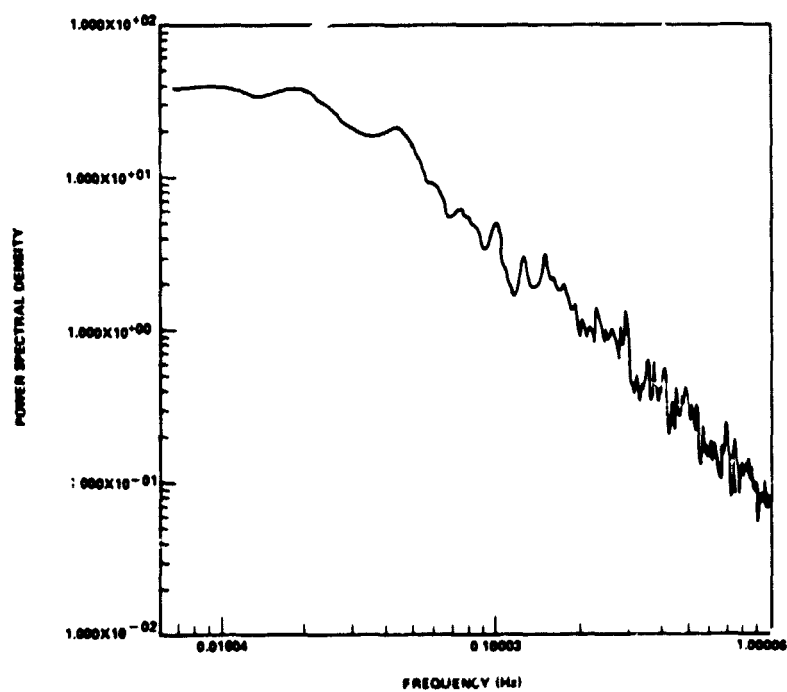

Figure 26. Power spectral density of lateral component (data taken at an elevation of 90 m, rms = 1.48 m/s).
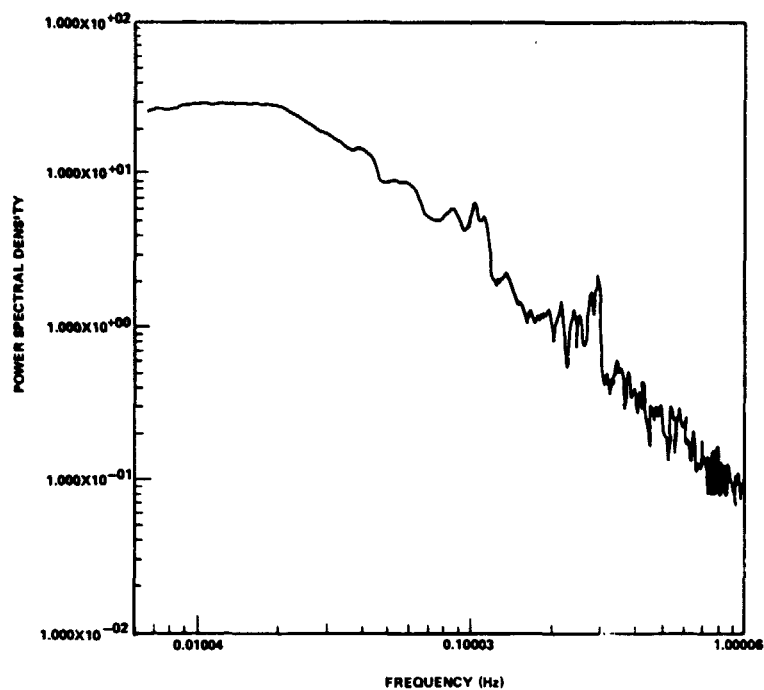
21

Figure 27. Power spectral density of lateral component (data
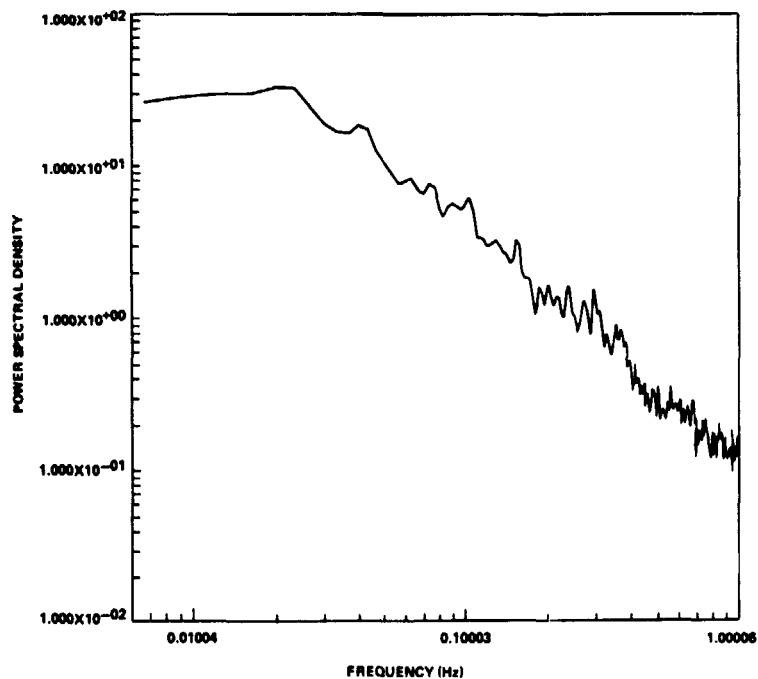taken at an elevation of 120 m, rms = 1.38 m/s).

Figure 28. Power spectral density of lateral component (data
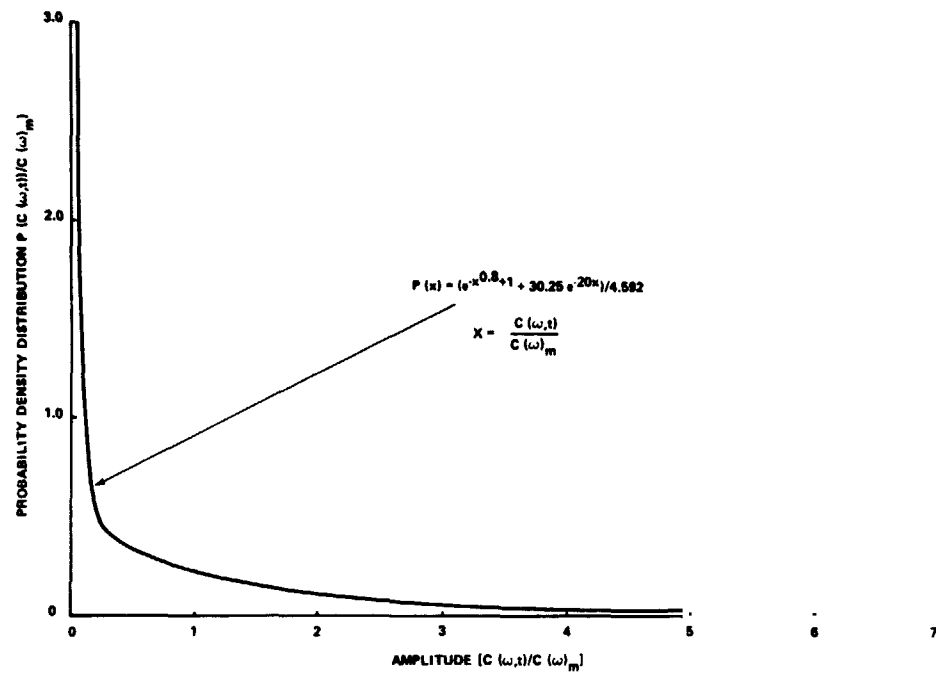taken at an elevation of 150 m, rms = 1.46 m/s).

PROBABILITY DENSITY DISTRIBUTION P (C (ω,t)/C (ω)$_m$)

$P(x) = (e^{-x^{0.8}+1} + 30.25\,e^{-20x})/4.582$

$X = \dfrac{C(\omega,t)}{C(\omega)_m}$

AMPLITUDE [C (ω,t)/C (ω)$_m$]

Figure 29. Probability density distribution of power spectral amplitudes.

x^2P(x)

$x^2 P(x):\quad X = \dfrac{C(\omega,t)}{C(\omega)_m}\ ;\ P(x) = (e^{-x^{0.8}+1} + 30.25\,e^{-20x})/4.582$
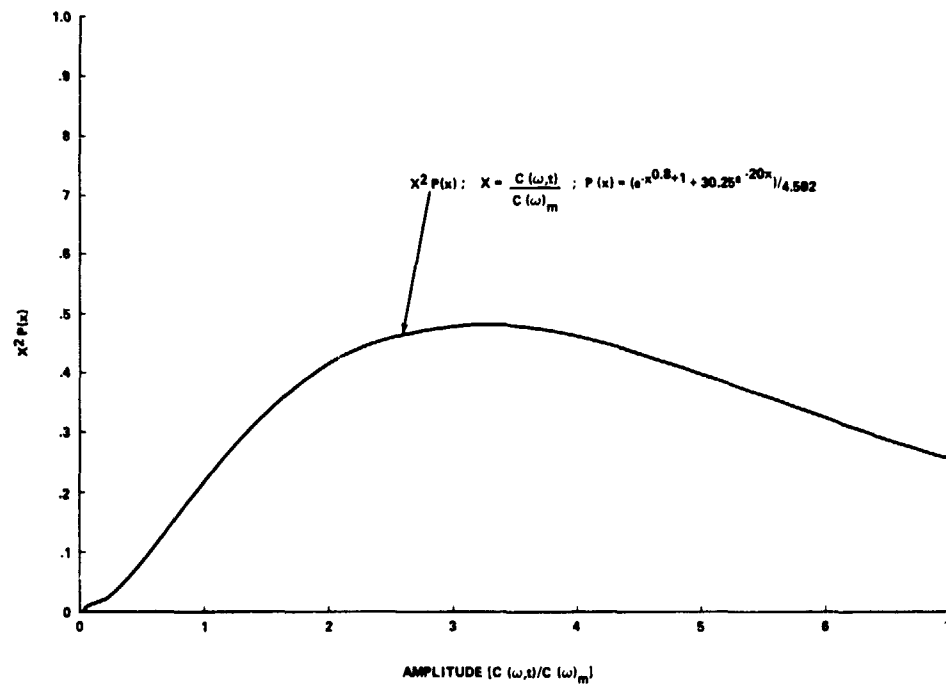
AMPLITUDE [C (ω,t)/C (ω)$_m$]

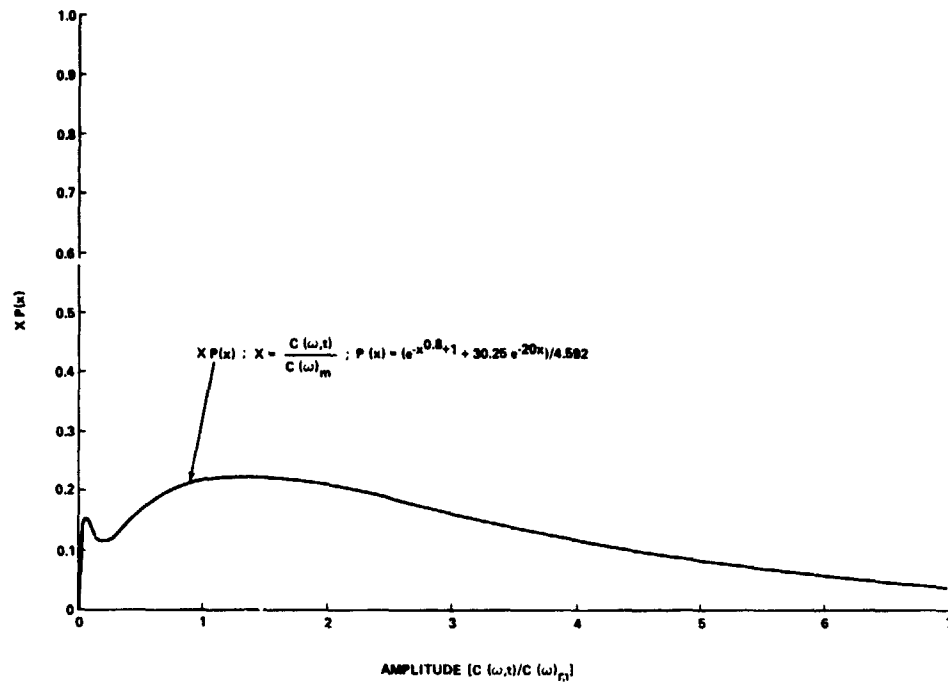Figure 30. Distribution of variance as a function of amplitude.

Figure 31. Distribution of mean spectral value as a function of amplitude.
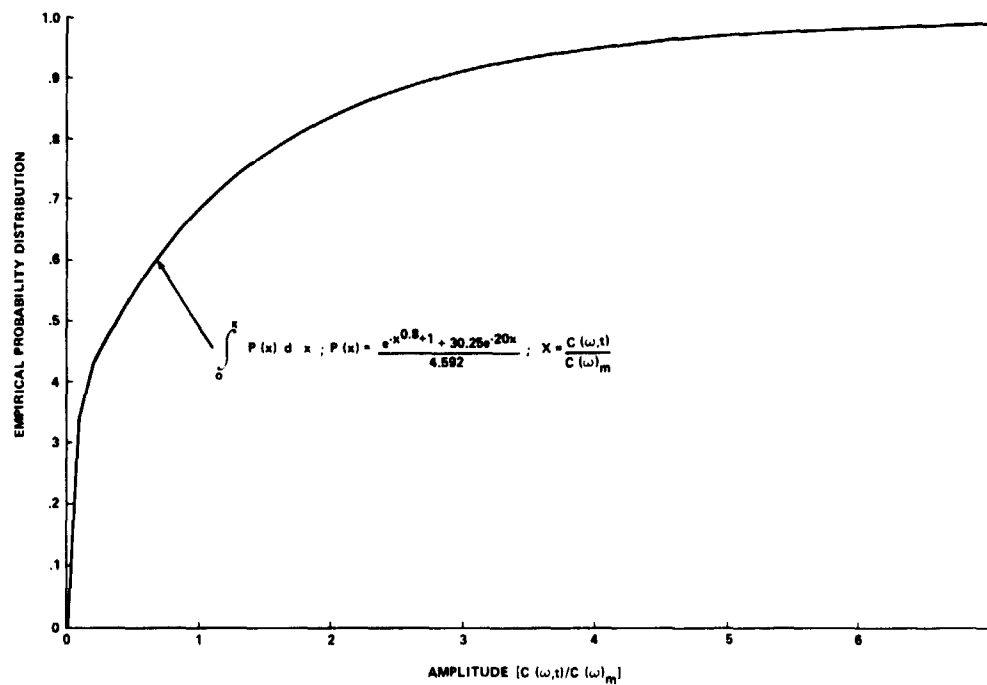

Figure 32. Empirical probability distribution of power spectral amplitudes.

24

REFERENCES

1.   Taylor, G. I.: Eddy Motion in the Atmosphere. Phil. Trans. of The Royal Society, A, Vol. CCSV, 1915, pp. 1-26.

2.   Taylor, G. I.: Observations and Speculations on the Nature of Turbulent Motion. Reports and Memoranda of the Advisory Committee for Aeronautics, No. 345, 1917.

3.   Taylor, G. I.: The Spectrum of Turbulence. Proceedings of The Royal Society, A, Vol. CLXIV, 1938, pp. 476-490.

4.   Cliff, William C. and Sandborn, Virgil A.: Measurements and A Model for Convective Velocities in The Turbulent Boundary Layer. NASA Technical Note D-7416, October 1973.
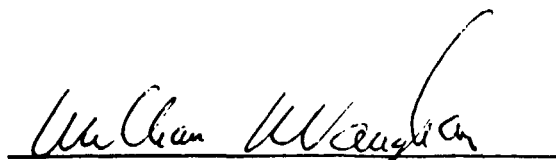
APPROVAL

MEASUREMENTS OF THE STOCHASTIC NATURE OF ATMOSPHERIC SPECTRAL AMPLITUDES

By William C. Cliff, George H. Fichtl,
Margaret Alexander, and Salvador Arias

The information in this report has been reviewed for security classification. Review of any information concerning Department of Defense or Atomic Energy Commission programs has been made by the MSFC Security Classification Officer. This report, in its entirety, has been determined to be unclassified.

This document has also been reviewed and approved for technical accuracy.

WILLIAM W. VAUGHAN
Chief, Aerospace Environment Division

CHARLES A. LUNDQUIST
Director, Space Sciences Laboratory